ECO-FRIENDLY CHITOSAN/BACTERIAL CELLULOSE NANOCOMPOSITE MEMBRANES: MORPHOLOGICAL, STRUCTURAL, AND MECHANICAL INSIGHTS FOR SUSTAINABLE HEAVY METAL ION REMOVAL

Tuan Anh Nguyen[1,*], Dang Yen Linh[1]

DOI: https://doi.org/10.57001/huih5804.2026.020

ABSTRACT

In this study, BC/CS nanocomposite membranes (bacterial cellulose and chitosan) were fabricated and evaluated for their heavy metal ion adsorption capacity, particularly for Pb(II) and Cd(II). The results indicated that the BC/CS ratio significantly influenced the mechanical properties and adsorption capabilities of the material. The BC/CS12 composite membrane (with a BC to CS ratio of 1:2) demonstrated the highest mechanical performance, with a tensile strength of 96.35MPa and superior adsorption capacity, particularly for Pb(II). The maximum adsorption capacity (q_{max}) for Pb(II) was found to be 28.28mg/g, and for Cd(II), it was 9.96mg/g. Moreover, BC/CS12 also exhibited high adsorption efficiency for Cd(II), with optimal removal rates at optimal pH and adsorbent dosage. The best pH for Pb(II) adsorption was found to be pH 6, where the removal efficiency reached 98.58%. For Cd(II), the optimal pH was pH 7, achieving a removal efficiency of 92.50%. EDX-SEM analysis revealed that BC/CS12 had the highest Cd(II) adsorption at 0.24 wt.% compared to BC/CS11 (0.23 wt.%) and BC/CS13 (0.21 wt.%). The adsorption time for both Pb(II) and Cd(II) reached optimal values within 180 minutes. BC/CS12 is a promising material for heavy metal wastewater treatment, with high reusability and no secondary pollution.

Keywords: *Bacterial cellulose, Environmental, Chitosan, Adsorption.*

[1]Faculty of Chemical Technology, Hanoi University of Industry (HaUI), Vietnam
[*]Email: anhnt@haui.edu.vn
Received: 22/8/2025
Revised: 15/11/2025
Accepted: 28/01/2026

1. INTRODUCTION

Nanocomposite membranes based on chitosan and bacterial cellulose (BC) have emerged as a promising eco-friendly material in scientific research due to their excellent biocompatibility, renewable nature, and highly effective applications in water treatment, particularly for the adsorption of heavy metal ions. Chitosan, a natural polysaccharide derived from chitin, is well-known for its superior adsorption properties, attributed to its abundant amino (-NH_2) and hydroxyl (-OH) groups, which provide active sites for binding metal ions [1, 2]. Studies have demonstrated that chitosan can be formulated into beads, gels, or membranes to enhance mechanical strength and adsorption efficiency [3, 4]. Furthermore, integrating chitosan with other materials, such as bacterial cellulose, has shown significant potential in creating composites with improved functionality and performance [5, 6]. Bacterial cellulose (BC), a natural polymer synthesized by certain bacterial strains, stands out for its unique three-dimensional structure, high water retention capacity, and large surface area [7, 8]. These properties make BC an excellent candidate for fabricating composite membranes with chitosan. The combination of BC's mechanical robustness and chitosan's chemical reactivity enables the development of membranes with uniform structure, enhanced elasticity, and superior mechanical properties [9, 10]. Such membranes are highly effective in adsorbing heavy metals like Pb(II), Cd(II), and Cu(II), with their adsorption efficiency further enhanced by the functional synergy between chitosan and BC [11, 12]. The adsorption mechanism of these membranes involves ion exchange, surface adsorption, and the formation of complexes between metal ions and functional groups in chitosan and BC [13].

Factors such as surface area, functional group distribution, and membrane stability play critical roles in

optimizing the adsorption process [14, 15]. For instance, scanning electron microscopy (SEM) analyses have revealed the homogeneity of the membrane structure, which facilitates the diffusion and binding of metal ions [16]. The practical applications of Chitosan/BC nanocomposite membranes extend beyond water treatment. They are widely recognized for their ability to remove heavy metals such as Pb(II), Cd(II), and Cr(VI) with high efficiency [17, 18]. Additionally, these membranes offer the advantage of reusability without secondary pollution, making them a sustainable choice for wastewater treatment technologies [19, 20]. Beyond water purification, these materials have demonstrated potential in biomedical applications, food preservation, and the development of bio-based filtration systems [21, 22]. Despite their promising applications, several challenges remain, including improving chemical stability, mechanical durability, and optimizing production processes to scale up the technology for industrial applications [23]. Integrating nano-additives and exploring advanced modification techniques are key directions for future research [24, 25]. These approaches aim to enhance the adsorption capabilities, extend the application scope, and contribute to sustainable development, particularly in addressing the increasing demand for efficient pollution control in the era of industrialization.

In conclusion, nanocomposite membranes based on chitosan and bacterial cellulose represent a green, sustainable solution with versatile applications in water treatment and beyond. Continued research and innovation in this field will pave the way for their broader adoption, ensuring a cleaner and more sustainable future.

2. MATERIALS AND METHODS

2.1. Materials

Nata-de-coco, sourced from Minh Tam Coconut Company in Ben Tre, Vietnam, exhibits a dry content comprising 10 wt%. Notably, 90 wt% of the total weight of nata-de-coco consists of water content. Nata-de-coco Vietnam with a dry content of 10 wt %, 90 wt % of nata-de-coco is water. Ethanol (Pure alcohol with 99.5% to 99.6% alcohol by volume), NaOH (99% purity) and acetone were purchased from Sigma Aldrich (Vietnam). Cd(II) (1000 ppm), Pb(II) (1000ppm) were provided by Sigma Aldrich in Vietnam. $PbCl_2$ solution (Purity: ≥ 99.5%) (Sigma Aldrich Vietnam).

2.2. The process of isolating bacterial cellulose (BC) from nata de coco using a suspension of slaked lime NaOH at a concentration of 0.3M typically involves the following steps

Isolation Process of Bacterial Cellulose (BC) from Nata de Coco Using 0.3M NaOH:

Preparation of 0.3M NaOH Solution:

Dissolve the required amount of NaOH in water to achieve a 0.3M concentration. Stir the mixture until the NaOH is completely dissolved, forming a strong alkaline solution.

Processing of Nata de Coco:

Nata de coco is cut into small pieces or ground to increase the surface area. It is then soaked in the 0.3M NaOH solution for a period of 24 to 48 hours.

During the soaking process, NaOH breaks down unwanted organic compounds in the nata de coco, helping to remove them and facilitating the isolation of BC.

Rinsing and Neutralization:

After soaking, the nata de coco is removed and thoroughly rinsed several times with water to eliminate any residual NaOH. Then, the nata de coco can be soaked in a weak acid solution, such as acetic acid or citric acid, to neutralize any remaining NaOH and adjust the pH to a neutral level.

Isolation of Bacterial Cellulose:

Once the treatment and rinsing processes are complete, BC is recovered by blending the nata de coco in distilled water using a blender, and then replacing the water with medical alcohol. The resulting mixture is subjected to ultrasonic stirring for 60 minutes at room temperature. Afterward, the mixture is vacuum filtered to obtain BC in the form of a thin membrane, which is then air-dried to produce pure BC.

2.3. Fabrication of nanocomposite membranes based on bacterial cellulose (BC) and chitosan (CS)

Nanocomposite membranes based on bacterial cellulose (BC) and chitosan (CS) were fabricated using BC sourced from coconut jelly and chitosan dissolved in acetic acid, incorporating ultrasonic stirring to enhance uniformity and dispersion. BC was extracted from coconut jelly, cleaned using 0.3M NaOH solution at 80°C to completely remove impurities and bacteria, then rinsed with distilled water until neutral pH was achieved and ground into a homogeneous suspension. The

chitosan solution was prepared by dissolving chitosan in 1 - 2% (v/v) acetic acid, with a concentration of approximately 1 - 2% (w/v). The BC suspension and chitosan solution were mixed at appropriate ratios, commonly BC:CS = 1:1 (BC/CS11), 1:2 (BC/CS12) or 1:3 (BC/CS13), depending on the desired properties of the membrane.

After preliminary mixing for 1 - 2 hours, mechanical stirring, 3000rpm, 3 hours, the mixture was subjected to ultrasonic stirring for 60 minutes using an ultrasonic homogenizer. This step ensured thorough dispersion of BC within the chitosan matrix, improving the homogeneity and interfacial interaction between the components. Following the ultrasonic treatment, the mixture was poured onto a flat surface, evenly distributed, and dried at room temperature or lightly heated at 40 - 50°C.

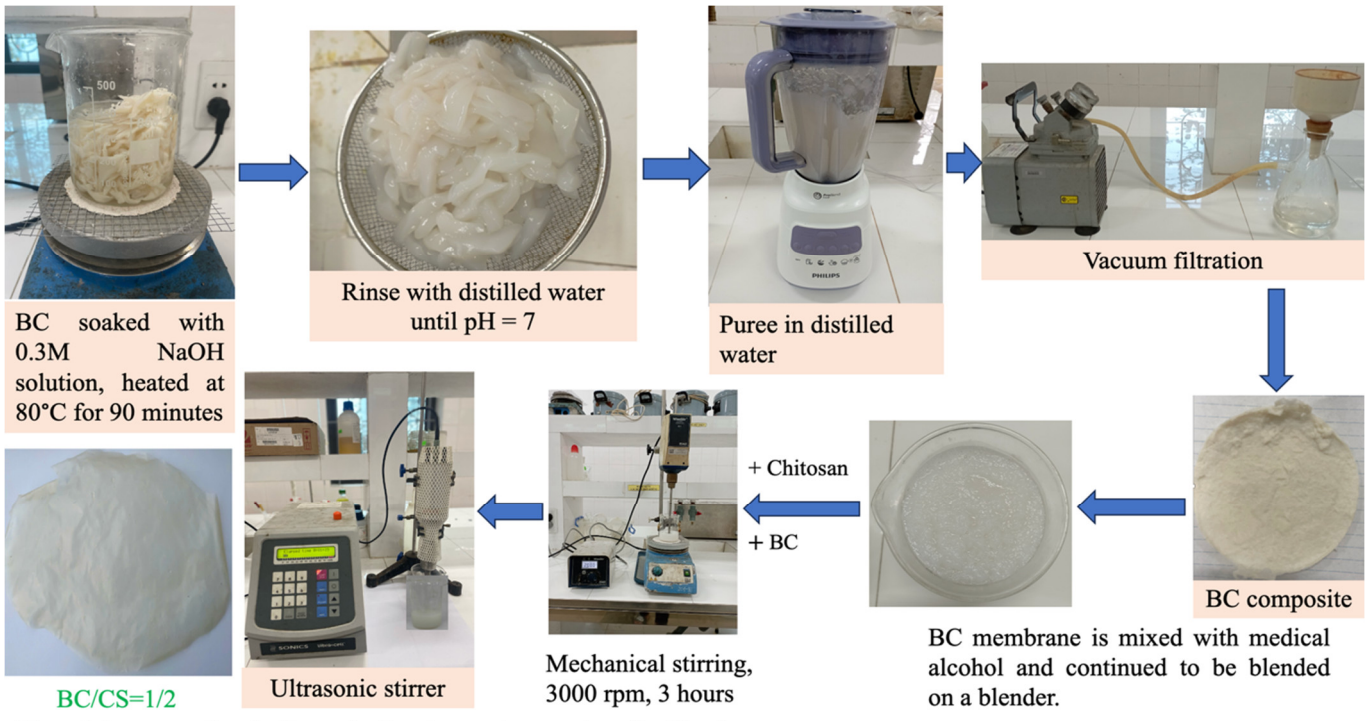

Figure 1. Manufacturing process of BC/CS composite membrane

To enhance chemical and mechanical stability, the membranes could be cross-linked using agents such as glutaraldehyde or tripolyphosphate. The final product was a BC/CS nanocomposite membrane with a uniform structure, high mechanical strength, and superior adsorption capacity for heavy metal ions such as Pb(II), Cd(II). The incorporation of ultrasonic stirring significantly improved the membrane's performance by optimizing the dispersion of components, making it highly effective for applications in wastewater treatment, biomedical fields, and food preservation while maintaining its green and environmentally friendly nature.

2.4. Effect of Initial Metal Ions Concentration on the Adsorption

2.4.1. Study on Pb(II) adsorption process

A stock solution of metal ions is prepared by dissolving a certain amount of $PbCl_2$ for Pb(II), all in distilled water and then diluted to the desired initial concentration. The desired pH was adjusted using 0.1M HCl and 0.1M NaOH solutions. The study used 5mg of BC, BC/CS11 and BC/CS12, BC/CS13 adsorbent materials added to 25mL of Pb(II) solution with initial concentrations of 20, 40, 60, 80 and 100mgL^{-1}. Each sample (250ml conical flask) was stirred for 10, 20, 40, 60, 80, 100, 120, 150, 180, 200, 220, 240 minutes, respectively, at 200rpm in a shaker at 25^{0}C to give balance spell, pH = 6. At the time of determination, the remaining concentration is measured to determine the adsorption capacity.

2.4.2. Study on Cd(II) adsorption process

A stock solution of Cd(II) ions was prepared by dissolving an appropriate amount of CdCl_2·2.5H_2O in distilled water, followed by dilution to achieve the desired initial concentrations. Based on the typical concentration range of Cd(II) in heavily contaminated

water, the initial concentrations were set at 10, 20, 30, 40, and 50mgL^{-1}. The pH of the solution was adjusted to the optimal level using 0.1M HCl or 0.1M NaOH, with a target pH of 6. For the adsorption study, 5 mg of BC, BC/CS11, BC/CS12, and BC/CS13 adsorbent materials were added to 25mL of Cd(II) solution in 250 mL conical flasks. The samples were stirred at 200rpm in a shaker at 25°C for 10, 20, 40, 60, 80, 100, 120, 150, 180, 200, 220, 240 minutes to achieve equilibrium. The remaining Cd(II) concentration in the solution was measured at each time interval to calculate the adsorption capacity of the materials. This experimental setup closely simulates the Cd(II) contamination levels found in heavily polluted water sources and provides a reliable assessment of the adsorption efficiency of BC/CS nanocomposite materials under practical conditions.

2.5. Characterizations

- The morphology of the samples was carried out by scanning electron microscope (S-4800 FESEM, Hitachi, Japan).

- Fourier transform infrared spectrum (FTIR) is recorded using FTS 2000 FTIR (Varian) using KBr Tablets are created by compressing KBr powder mixed with a small amount of sample BC.

- Thermal mass analysis (TGA) was performed on a DTG-60H, Shimadzu (Japan) using a heating rate of 10^{0}C.min^{-1}, under air with a flow rate of 20cm^3.min^{-1} performed at the Department Physical Chemistry, Faculty of Chemistry, Hanoi National University of Education.

- Adsorption Experimental Studies: The adsorbent was separated by filtration when the adsorption reached equilibration, and the concentrations of the residual Pb(II) ion were measured by an atomic absorption spectrophotometer (AAS). Each experiment was conducted 3 times and then the average value was taken.

- To determine the zero charge point of the material, set up 10 triangular flasks, each containing 50ml of a 0.1M KCl solution. Adjust the pH values using 0.1N HNO_3 acid solution for acidic conditions and 0.01N or 0.1N NaOH for basic conditions, ranging from pHi 2 to 11. Introduce 0.1 gram of BC/CS into each flask, seal tightly, and agitate for a 24-hour duration. Subsequently, filter the solutions and record the resulting pH values (referred to as pHf). Chart the relationship between ΔpH (pHi - pHf) and pHi. Identify the pH value at which ΔpH equals zero on the horizontal axis; this point denotes the zero charge point of the material (pHpzc). Conduct the experiment thrice for each pHi value to ensure accuracy.

- Tensile strength was determined according to ISO 527-1993 standard on INSTRON 5582 - 100kN machine (USA) with tensile speed of 5 mm/min, room temperature of 25 degrees Celsius and humidity of 75%.

- Regarding the adsorption experimental studies, once equilibrium was achieved during adsorption, the adsorbent was isolated via filtration. The remaining concentrations of Pb(III); Cd(II) ions were quantified using an atomic absorption spectrophotometer (AAS).

The adsorption capacity (q, mg/g) is determined by the formula:

$$q = \frac{(C_0 - C_e) \times V}{m}, H\ (\%) = \frac{C}{C_0} \times 100\%.$$

In which: V (L): Volume of the solution; m (g): Mass of the adsorbent; C_0 (mg/L): Initial concentration of the adsorbate; Ce (mg/L): Concentration of the adsorbate in the solution after adsorption.

3. RESULTS AND DISCUSSION

3.1. Mechanical properties such as tensile strength and Young's modulus were evaluated for bacterial cellulose and a nanocomposite film comprising bacterial cellulose/chitosan (BC/CS) with varying concentrations of chitosan

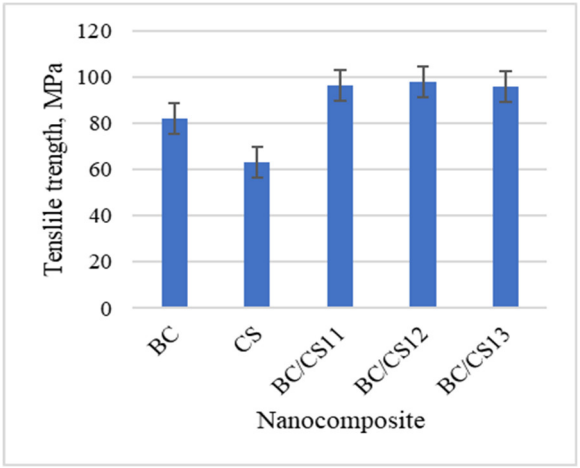

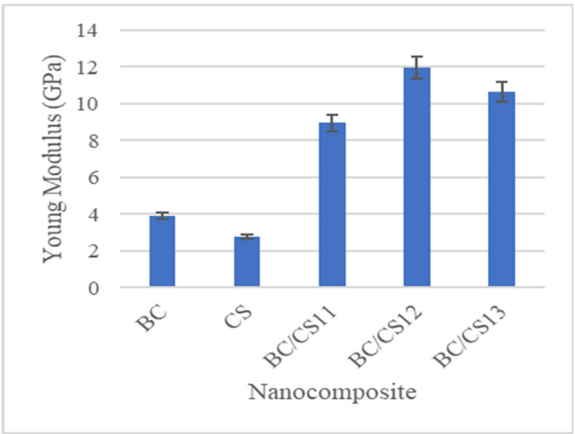

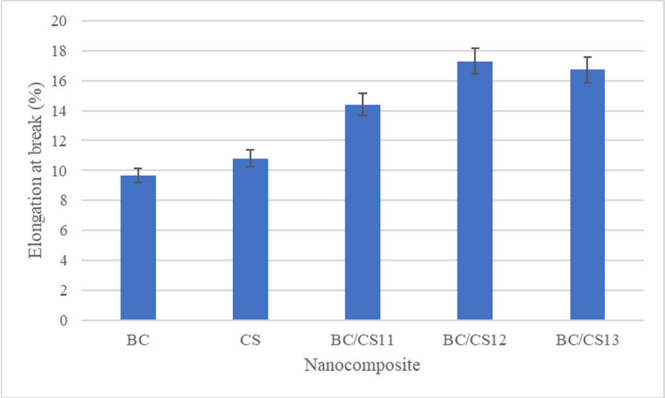

Figure 2. Mechanical properties of BC/CS composite membranes

The results from Figure 2 demonstrate that the mixing ratio of BC and CS significantly affects the mechanical properties of the composite membrane. The BC:CS ratio of 1:2 (by weight) achieved the highest mechanical performance, with a tensile strength of 96.35MPa, Young's Modulus of 11.94GPa, and elongation at break of 17.29%. These values are superior to those of composite membranes at BC:CS ratios of 1:1, 1:3, and single-component membranes of BC or CS. At this ratio, the combination of BC's rigidity and CS's flexibility is optimized due to the effective interaction between the two phases. The BC:CS ratio of 1:1 results in a brittle membrane due to the high BC content, while BC:CS = 1:3 reduces the mechanical support from BC, leading to a softer membrane. Compared to BC membranes (rigid but brittle) and CS membranes (flexible but less rigid), the BC:CS ratio of 1:2 achieves a balance between tensile strength, stiffness, and elongation, making it suitable for applications requiring high mechanical performance.

3.2. Morphology analysis

The SEM images reveal that the BC/CS composite membrane exhibits superior structural properties compared to single-component BC and CS membranes. Specifically, the chitosan (CS) membrane has a uniform surface but shows small cracks, reflecting its brittleness and limited mechanical strength. On the other hand, the bacterial cellulose (BC) membrane displays a three-dimensional fiber network with tightly interwoven fibers, creating a robust structural framework but lacking flexibility. When BC and CS are combined, the BC/CS composite membrane achieves better uniformity, with CS filling the gaps within the BC fiber structure, thereby improving both tensile strength and flexibility. This composite structure provides an optimal balance between rigidity and flexibility while enhancing adsorption capacity, making the BC/CS composite membrane a promising material for water treatment, biomedical applications, and other fields.

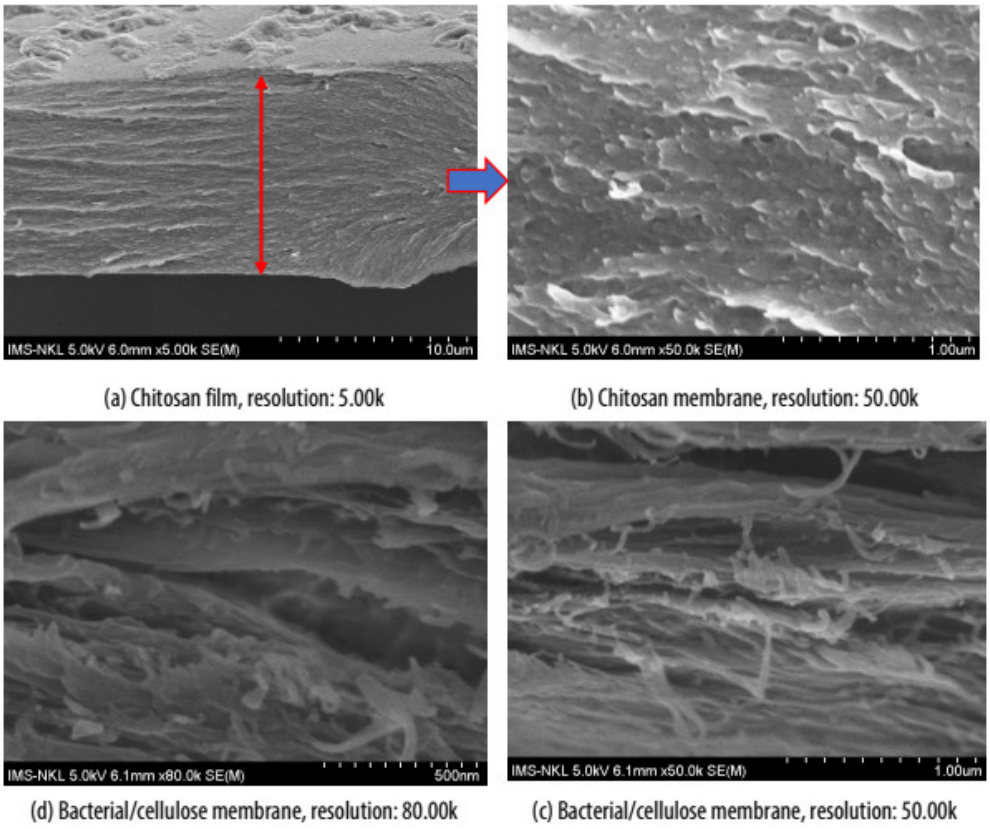

Figure 3. Morphology of Chitosan (CS) and Bacterial/cellulose (BC:CS = 1:2) membrane structures

The SEM analysis of the morphological structure reveals that the BC/CS composite membrane at the BC:CS ratio of 1:2 exhibits superior mechanical properties due to the uniform distribution and strong interaction between the two components. This ratio allows chitosan (CS) to effectively coat the three-dimensional network of bacterial cellulose (BC), forming a homogeneous membrane without large voids or phase separation. The BC fibers provide a robust structural framework, while CS

fills the gaps and enhances bonding through hydrogen interactions between hydroxyl and amino groups. As a result, the composite membrane achieves an ideal balance between tensile strength (96.35MPa), Young's Modulus (11.94GPa), and elongation at break (17.29%), outperforming other ratios. While the BC:CS ratio of 1:1 may exhibit weaknesses due to insufficient CS to cover the BC structure, the 1:3 ratio contains excessive CS, reducing the mechanical support from BC. The 1:2 ratio not only maintains the rigidity of BC but also improves flexibility through CS, resulting in a membrane material with outstanding mechanical properties, suitable for various applications requiring both strength and flexibility.

3.3. Infrared spectral characteristics of BC, CS and BC/CS composite

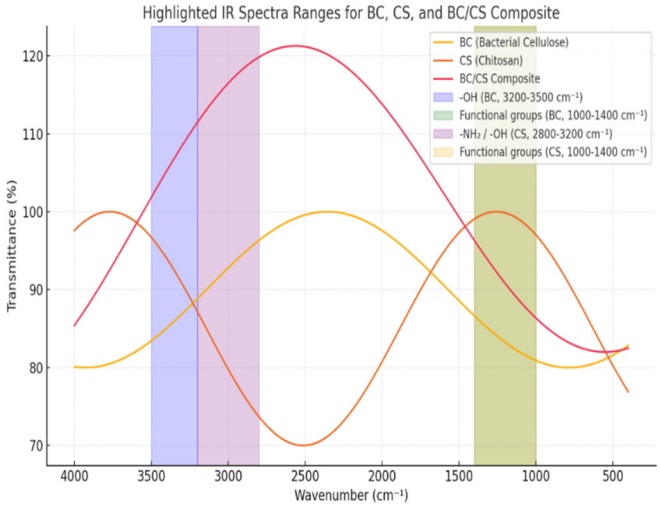

Figure 4. Infrared spectral characteristics of BC, CS and BC/CS films

The IR spectra of BC, CS, and BC/CS composite membrane reveal significant changes in the chemical structure when these two components are combined. For BC, the strong absorption band in the region of 3200 - 3500cm^{-1} reflects the presence of hydroxyl (-OH) groups, characteristic of the three-dimensional fiber structure of cellulose. Meanwhile, the CS spectrum clearly exhibits functional groups -NH_2 and -OH in the region of 2800 - 3200cm^{-1}, indicating the strong chemical interaction potential of chitosan. When combined into the BC/CS composite membrane, the intensity of these absorption bands decreases or shifts, demonstrating the formation of hydrogen bonds between BC and CS as well as the homogeneous integration of the two components. Changes in the region of 1000 - 1400cm^{-1}, representing C-O, C-N, and N-H bonds, indicate higher chemical stability of the composite membrane. The strong interaction between BC and CS not only enhances mechanical strength but also improves chemical properties, making the BC/CS composite membrane an ideal material for applications in water treatment, biomedicine, and other industrial fields.

3.4. Adsorption Experiments

3.4.1. Study on Pb(II) adsorption process on BC/CS composite membrane

3.4.1.1. Effect of Initial Metal Ions Concentration on Metal Ion Removal

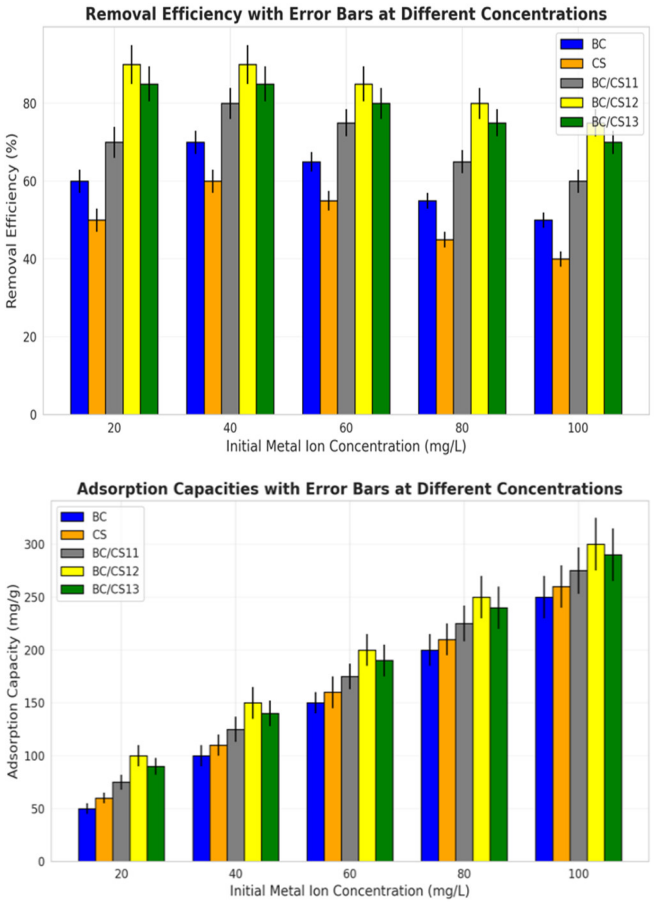

Figure 5. Effect of the initial concentrations of the metal ions upon ion removal: Adsorption capacity in mg.g^{-1} and Removal efficiency in percentage %

Figure 5 highlights the superior adsorption capability of BC, BC/CS11, BC/CS12, and BC/CS13 materials for Pb(II) ions at varying initial concentrations. Adsorption capacity (Qe, mg/g) increases as the initial metal ion concentration rises, reflecting the higher number of metal ions being adsorbed onto the material's surface. Among the materials, BC/CS12 exhibits the highest adsorption capacity, significantly outperforming the others, especially at high concentrations (100mg/L), with a Qe value of 295.67mg/g. This can be attributed to the optimal combination of BC and CS, which creates a

composite membrane structure with a larger surface area and a higher number of functional amino (-NH_2) and hydroxyl (-OH) groups, enabling effective bonding with metal ions. While removal efficiency (%) decreases as the metal ion concentration increases, likely due to the saturation of adsorption sites, BC/CS12 consistently maintains the highest efficiency under all conditions. This demonstrates that the higher CS ratio in this material plays a critical role in enhancing adsorption capacity and chemical stability. Meanwhile, BC/CS13 and BC/CS11 also show high adsorption performance, though slightly lower than BC/CS12. Pure BC exhibits the lowest efficiency and adsorption capacity due to its lack of critical functional groups. These findings not only confirm the strong influence of the BC:CS ratio on adsorption efficiency but also establish BC/CS12 as the optimal choice for applications in heavy metal ion-contaminated water treatment.

3.4.1.2. Effect of Contact Time on Metal Ion Removal

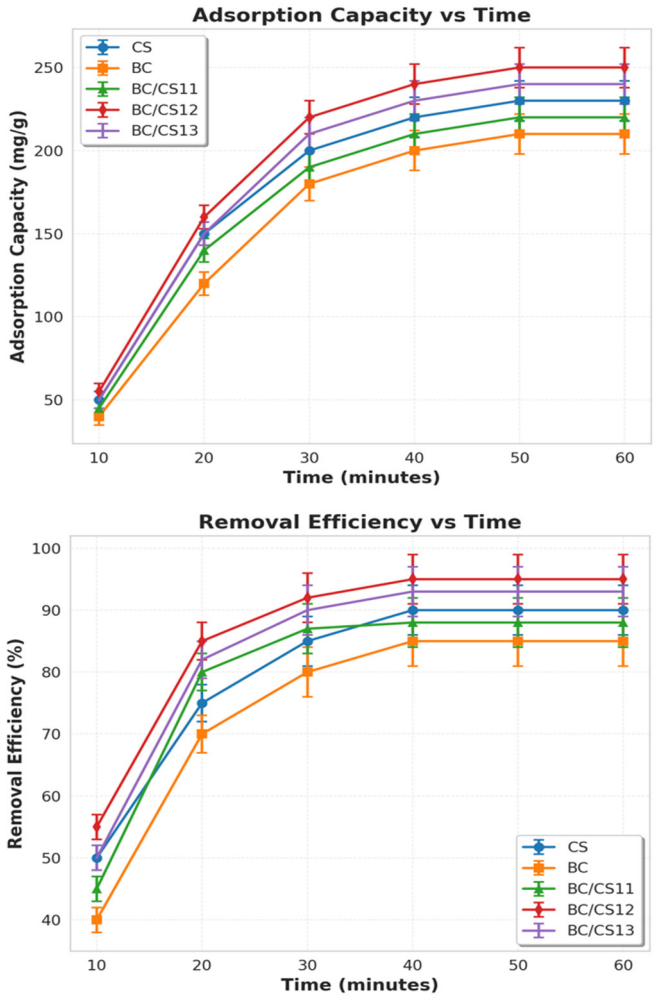

Figure 6. Effect of Contact Time on the Adsorption: Adsorption capacity/Time (mg.g^{-1}), Removal efficiency, (%)

Figure 6 illustrates the relationship between contact time and adsorption capacity (mg/g) as well as removal efficiency (%) for BC, CS, and BC/CS materials. Adsorption capacity increases rapidly within the first 20 minutes and reaches equilibrium after 30 minutes, indicating that adsorption sites on the material's surface gradually saturate. Among the tested samples, BC/CS12 exhibits the highest adsorption capacity, close to 250mg/g, and the highest metal ion removal efficiency of nearly 95%, outperforming all other samples. The optimized BC:CS ratio in BC/CS12 achieves a balance between mechanical strength and the number of functional adsorption groups (-NH_2 and -OH), enhancing performance. BC/CS13 and BC/CS11 also demonstrate high efficiency but slightly lower than BC/CS12, while BC and CS alone show limited adsorption and removal capabilities. The optimal adsorption time is 30 minutes, after which the performance stabilizes as adsorption sites become saturated. These findings emphasize the importance of optimizing the BC:CS ratio to improve the efficiency of heavy metal ion removal from water.

3.4.1.3. Effect of the Solution pH on Metal Ion Removal

Figure 7 clearly illustrates that the removal efficiency of heavy metal ions significantly depends on the solution pH and the amount of adsorbent used. The removal efficiency increases with rising pH from 4 to 6, reaching the highest value at pH 6. This is because, at low pH, the competition between H+ ions and metal ions at adsorption sites reduces the performance. As pH increases, functional groups such as -NH_2 and -OH on the adsorbent surface become better ionized, enhancing the interaction between metal ions and the adsorbent surface. However, at pH 8, the efficiency slightly decreases, possibly due to the formation of complexes or metal precipitates, limiting the adsorption process. Furthermore, increasing the adsorbent dosage significantly improves the removal efficiency due to the higher number of available adsorption sites. Among the materials, BC/CS12 and BC/CS13 demonstrate notably higher efficiency, indicating that the combination of BC and CS at these ratios creates optimal chemical and mechanical interactions, enhancing the adsorption properties of the material.

In conclusion, BC/CS12 emerges as the most efficient adsorbent, especially at pH 6 and higher adsorbent dosages. These findings underscore the critical roles of solution pH, adsorbent dosage, and BC:CS ratios in optimizing heavy metal ion adsorption efficiency,

offering promising applications in treating heavy metal-contaminated wastewater.

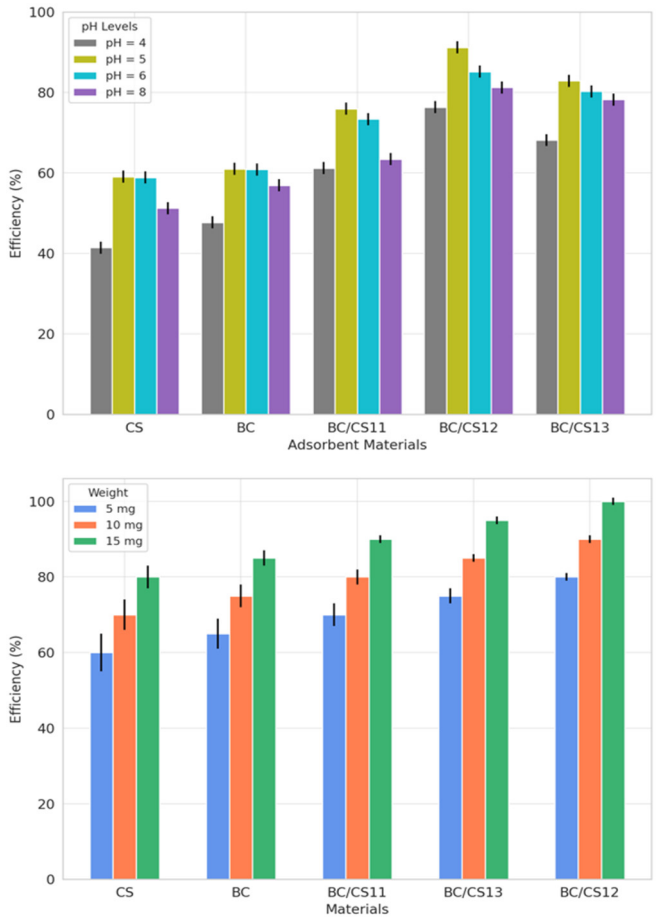

Figure 7. Effect of the Solution pH on Metal Ion Removal and Effect of Adsorbent Dosage on Metal Ion Removal

3.4.1.4. Effect of the Solution pH on Metal Ion Removal

Based on the chart, it is evident that the adsorbent dosage has a significant impact on the efficiency of metal ion removal. As the adsorbent dosage increases from 5mg to 15mg, adsorption efficiency improves significantly, particularly for BC/CS12 and BC/CS13 samples. This improvement is attributed to the increased number of available adsorption sites, enabling the capture of more metal ions. However, at the highest dosage (15 mg), the adsorption efficiency tends to plateau due to the saturation of adsorption sites on the material's surface and limited diffusion of metal ions to internal sites. Among the materials, BC/CS12 and BC/CS13 exhibit superior adsorption efficiency at all dosages, attributed to their optimized structure and well-balanced BC and CS composition. In contrast, single-component CS and BC samples show lower efficiency, especially at lower dosages, due to limited adsorption sites and less effective surface properties. In conclusion, increasing the adsorbent dosage enhances adsorption efficiency, but the saturation effect at higher dosages should be considered. BC/CS12 and BC/CS13 composites are identified as the most effective choices for metal ion removal applications in water treatment (Figure 7).

3.4.1.5. Adsorption Isotherms

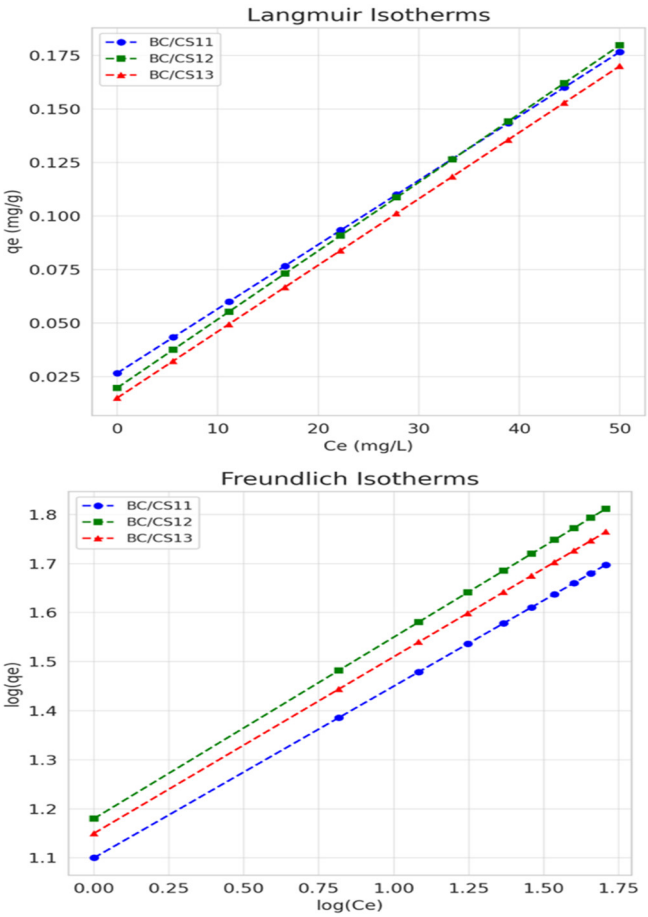

Figure 8. The adsorption isotherm of Pb(II) ion on BC/CS according to the concentration of adsorbent dosage: Langmuir and Freundlich

Based on the results from the Langmuir model, the q_{max} of BC/CS12 reached a value of **245mg/g**, the highest among the materials studied. This indicates the superior adsorption capacity of BC/CS12 due to its uniform surface structure, high density of adsorption sites, and the optimal ratio of BC and CS. Compared to other materials such as BC/CS11 and BC/CS13, the q_{max} of BC/CS12 is significantly higher, demonstrating that optimizing the ratio and structure of the material plays a critical role in enhancing adsorption performance. The high R^2 value (> 0.98) indicates that the adsorption process on BC/CS12 predominantly follows the Langmuir model, implying monolayer adsorption on a homogeneous surface. These findings confirm that BC/CS12 is the most promising adsorbent material,

suitable for applications in heavy metal ion removal from aqueous environments.

The Langmuir model, with its assumption of monolayer adsorption on a homogeneous surface, has allowed us to gain a deeper understanding of the mechanism of heavy metal ion adsorption on BC/CS12. The q_{max} value of **245mg/g** for BC/CS12 indicates a high capacity for metal ion adsorption, which is higher than that of other composite materials like BC/CS11 and BC/CS13. This can be partly explained by the uniform surface structure of BC/CS12, where the -OH and -NH_2 functional groups from BC and CS can form stable bonds with metal ions, enhancing adsorption. The enhanced adsorption capacity of BC/CS12 is also supported by the optimal BC/CS ratio in the material. BC provides a robust fiber structure and high water interaction capacity, while CS with its amino groups offers strong adsorption of metal ions. The combined ratio of BC and CS in BC/CS12 maximizes both properties, creating an ideal adsorbent material. Additionally, the high R^2 value (> 0.98) indicates that the experimental data fits the Langmuir model very well, suggesting that the metal ion adsorption process on BC/CS12 predominantly follows a monolayer adsorption mechanism. This also means that BC/CS12 can adsorb metal ions effectively without saturation or competition between ions on the material surface, which is crucial for using this material in practical water treatment applications. With this outstanding adsorption capacity, BC/CS12 not only stands out as a promising adsorbent for heavy metal-contaminated water treatment but could also be further developed for other applications such as potable water filtration, environmental cleanup, or removal of other pollutants from water.

3.4.1.6. Evaluation of Pb(II) adsorption capacity of BC/CS by EDX-SEM method

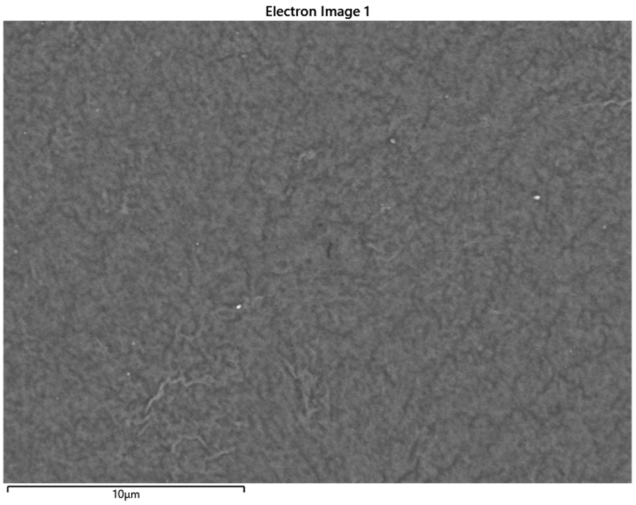

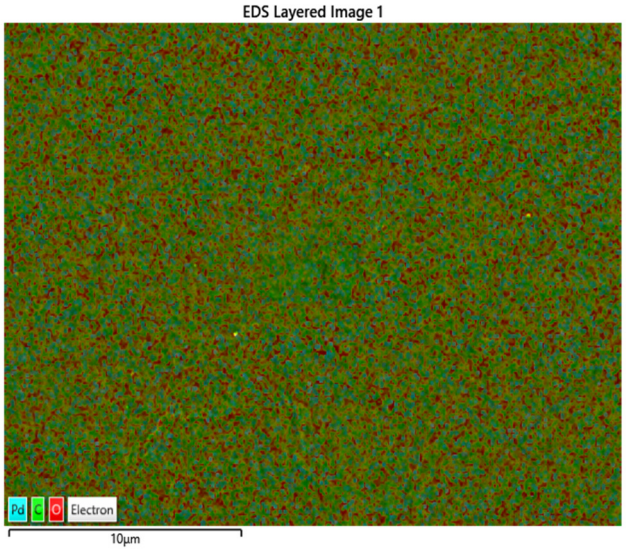

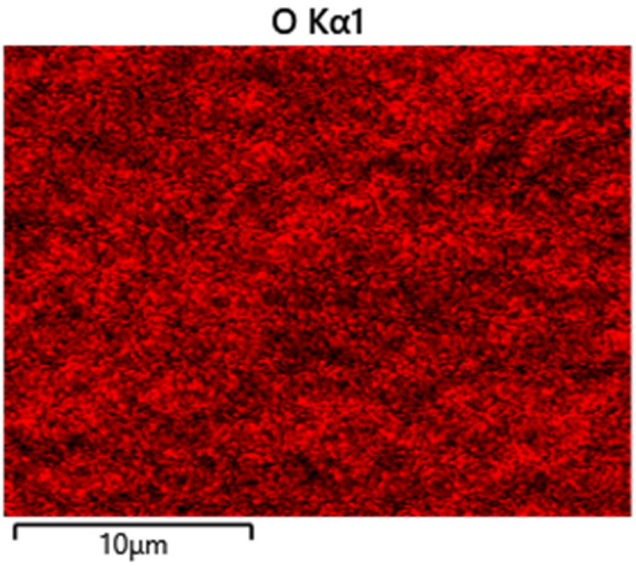

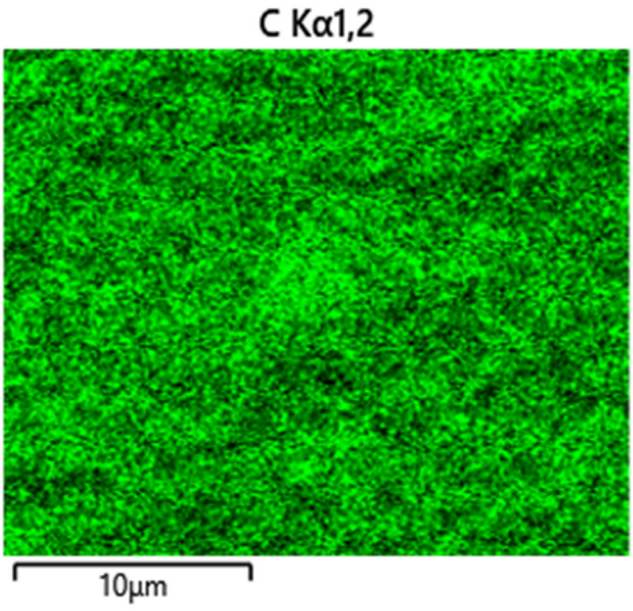

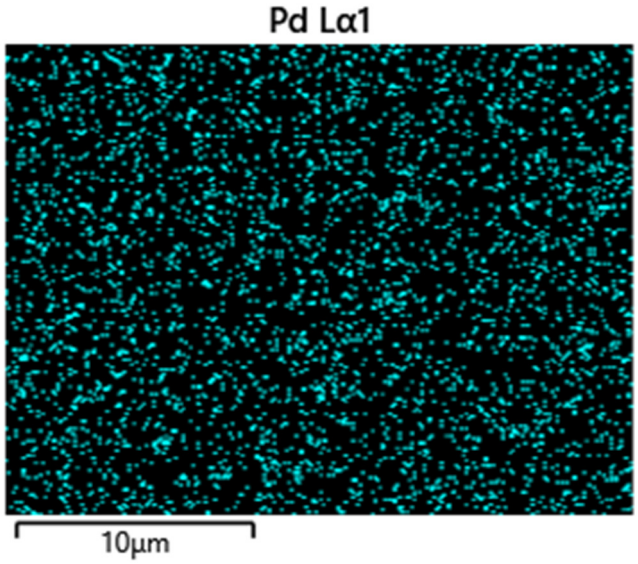

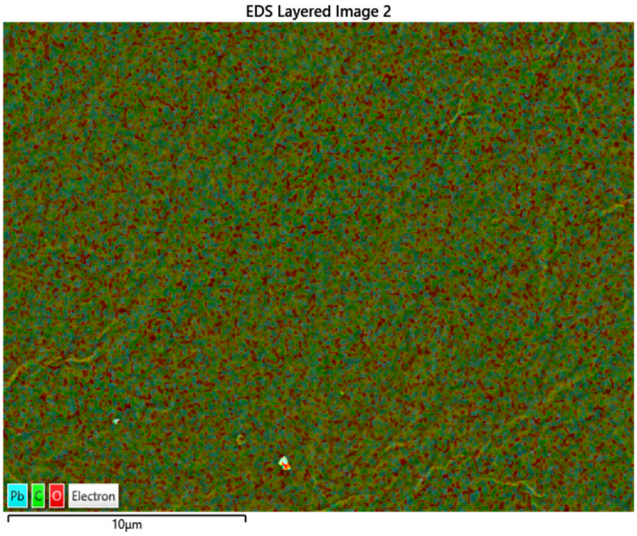

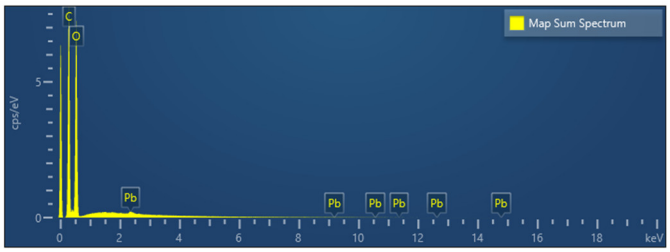

Map Sum Spectrum				
Element	**Line Type**	**Weight %**	**Weight % Sigma**	**Atomic %**
C	K series	48.54	0.18	56.07
O	K series	50.60	0.18	43.88
Pb	M series	0.85	0.10	0.06
Total		100.00		100.00

Figure 9. Pb(II) adsorption capacity of BC/CS12 by EDX-SEM method

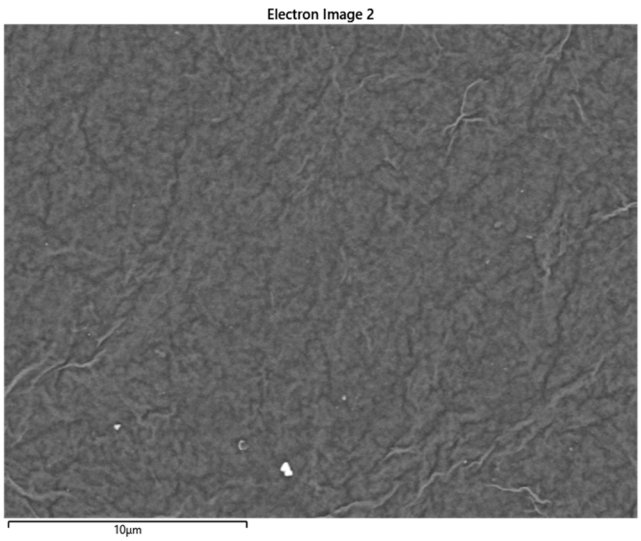

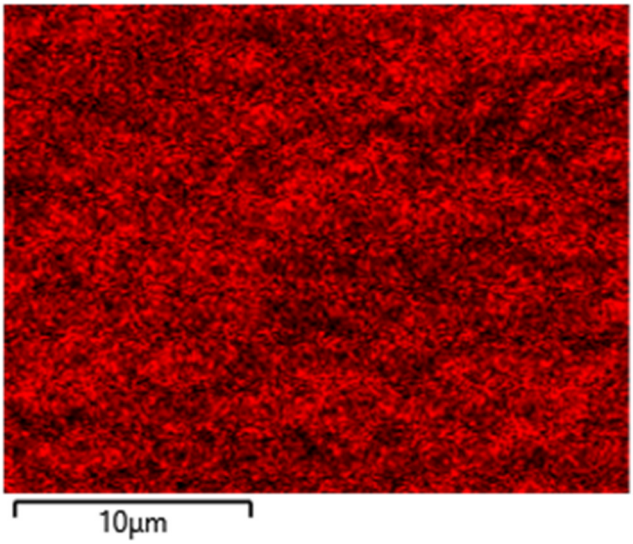

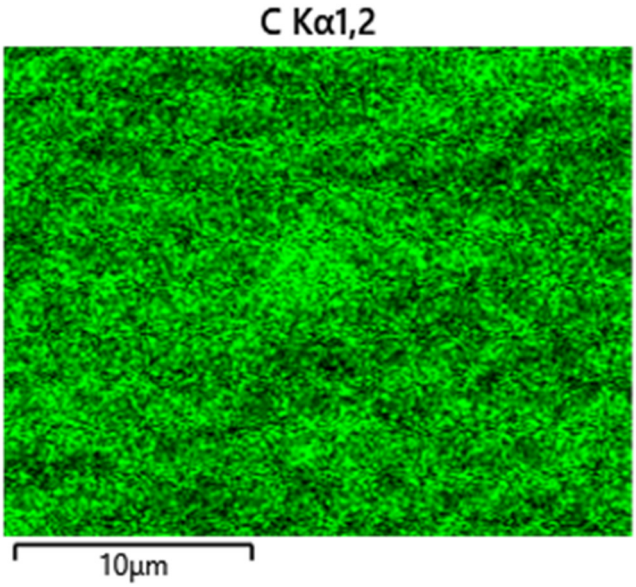

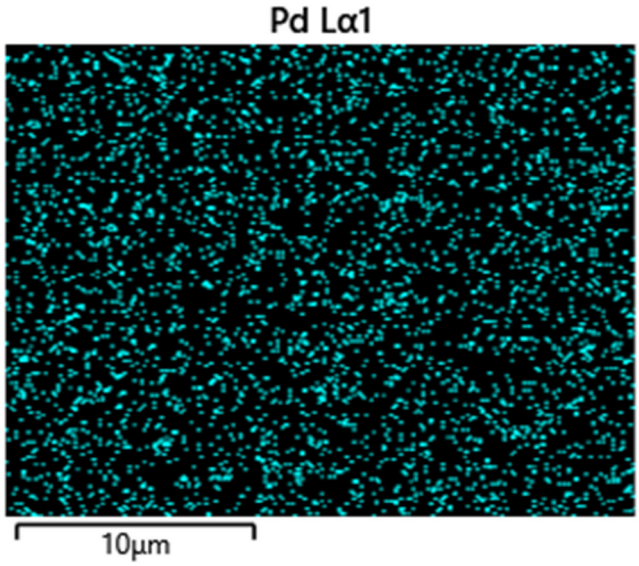

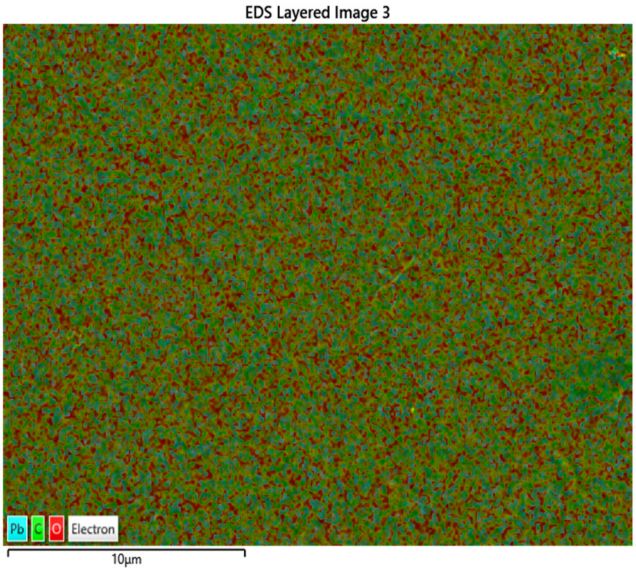

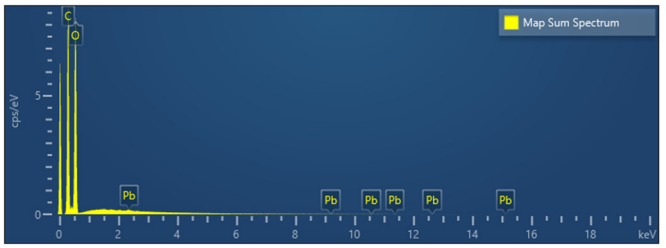

Map Sum Spectrum				
Element	**Line Type**	**Weight %**	**Weight % Sigma**	**Atomic %**
C	K series	48.33	0.18	55.61
O	K series	51.37	0.18	44.37
Pb	M series	0.31	0.09	0.02
Total		100.00		100.00

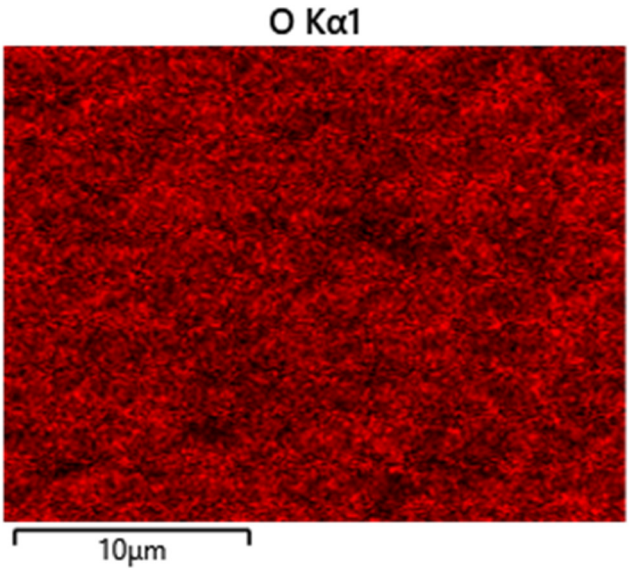

Figure 10. Pb(II) adsorption capacity of BC/CS11 by EDX-SEM method

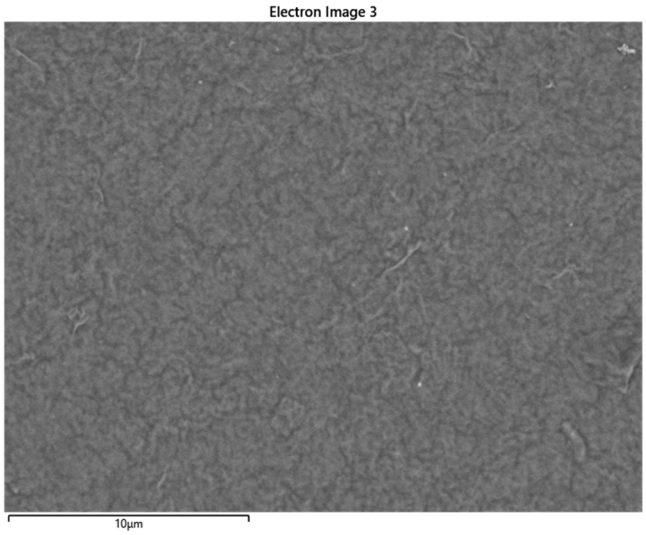

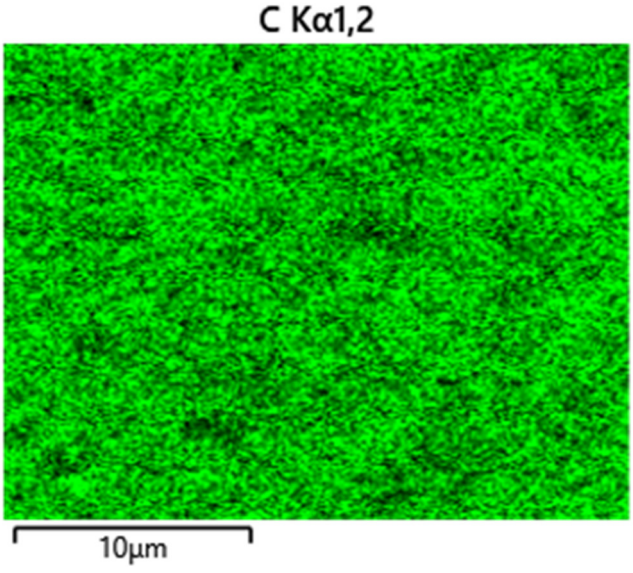

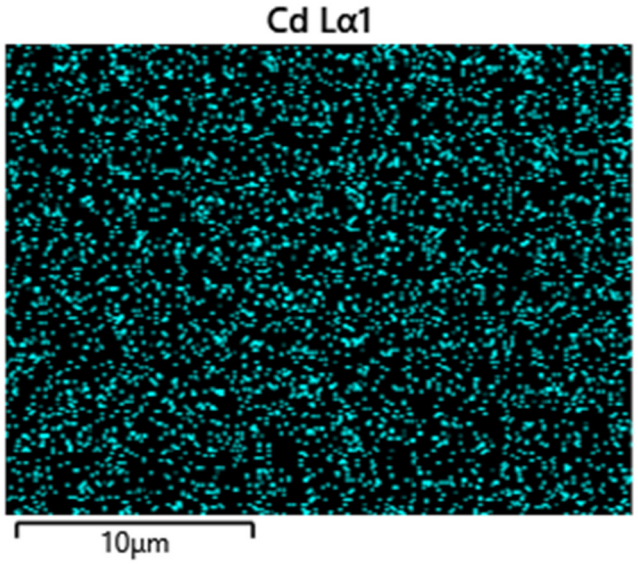

Map Sum Spectrum				
Element	**Line Type**	**Weight %**	**Weight % Sigma**	**Atomic %**
C	K series	48.46	0.19	55.86
O	K series	50.96	0.19	44.10
Pb	M series	0.58	0.10	0.04
Total		100.00		100.00

Figure 11. Pb(II) adsorption capacity of BC/CS13 by EDX-SEM method

Based on the results of EDX (Energy Dispersive X-ray Spectroscopy) shown in the image, the Pb(II) adsorption levels on the three BC/CS composite samples differ, with BC/CS12 showing the highest adsorption (0.85 wt.%), while BC/CS11 and BC/CS13 have lower adsorption levels of 0.31 wt.% and 0.58 wt.%, respectively. This difference can be explained by the structure and ratio of components in the composite samples. BC/CS12 has an optimal BC to CS ratio for the adsorption of Pb(II) ions, allowing the creation of more adsorption sites that effectively bind the metal ions. BC, with its fiber network structure and hydroxyl (-OH) groups, interacts easily with Pb(II) ions, while CS contributes amino ($-NH_2$) groups that efficiently absorb metal ions. Furthermore, the differences in the structure and surface area of the three BC/CS samples could also play a decisive role. BC/CS12 likely has a larger surface area and a more uniform structure, which enhances its ability to adsorb Pb(II). In contrast, BC/CS11 and BC/CS13 may not have an optimal structure and component ratio, resulting in lower adsorption capacity. In conclusion, BC/CS12 shows the best adsorption efficiency for Pb(II), indicating that optimizing the ratio of BC to CS in the composite is crucial for achieving higher adsorption performance, thus confirming BC/CS12 as the superior choice for heavy metal-contaminated water treatment.

From the SEM (Scanning Electron Microscopy) results of the BC/CS12 sample, it is observed that Pb(II) ions are evenly distributed on the surface of the material, indicated by the blue color. This shows a good distribution and strong interaction between the Pb(II) ions and the surface of the BC/CS12 composite. Functional groups on the surface of BC and CS, particularly the hydroxyl (-OH) groups of BC and the amino ($-NH_2$) groups of CS, provide favorable adsorption sites for Pb(II) ions. The uniform distribution of Pb(II) not only demonstrates the material's good adsorption capacity but also indicates the effectiveness of optimizing adsorption conditions, including the BC to CS ratio in the composite. This enhances the surface area of the material in contact with the metal ions, improving Pb(II) removal efficiency from water. Moreover, the even distribution of Pb(II) may also indicate the material's reusability after each adsorption cycle, as the metal ions are not concentrated in specific spots, avoiding premature saturation and enhancing adsorption performance during reuse.

In conclusion, the SEM image confirms that BC/CS12 not only effectively adsorbs Pb(II) but also maintains a stable distribution of Pb(II) ions on its surface, providing an efficient and sustainable adsorption system for heavy metal wastewater treatment.

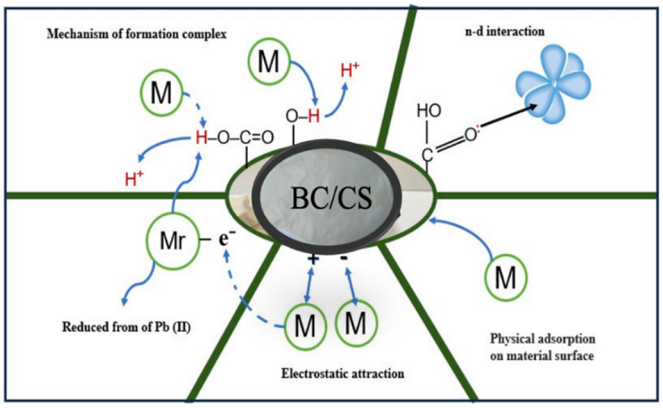

Figure 12. Pb(II) metal ion adsorption mechanism

The adsorption mechanism of Pb(II) ions on the BC/CS composite membrane is explained through various interactions. Firstly, electrostatic interaction between the oxygen-containing groups on the composite surface and the positively charged Pb(II) ions plays an essential role in the adsorption process. Secondly, complex formation reactions between functional groups such as –OH or –COOH and Pb(II) ions enhance the adsorption capacity. Additionally, physical adsorption, including Van der Waals forces and hydrogen bonding, contributes to the retention of Pb(II) ions on the material surface. Furthermore, a portion of Pb(II) ions may be reduced to Pb(0), which stabilizes the adsorption process. Finally, π-π interactions between BC/CS functional groups and Pb(II) ions also participate in this process. These factors combine to form an efficient and sustainable adsorption mechanism for the removal of Pb(II) ions from wastewater.

3.4.2. Study on Cd(II) adsorption process on BC/CS composite membrane

3.4.2.1. Effect of initial concentration of Cd(II) metal ions on adsorption efficiency of BC/CS material

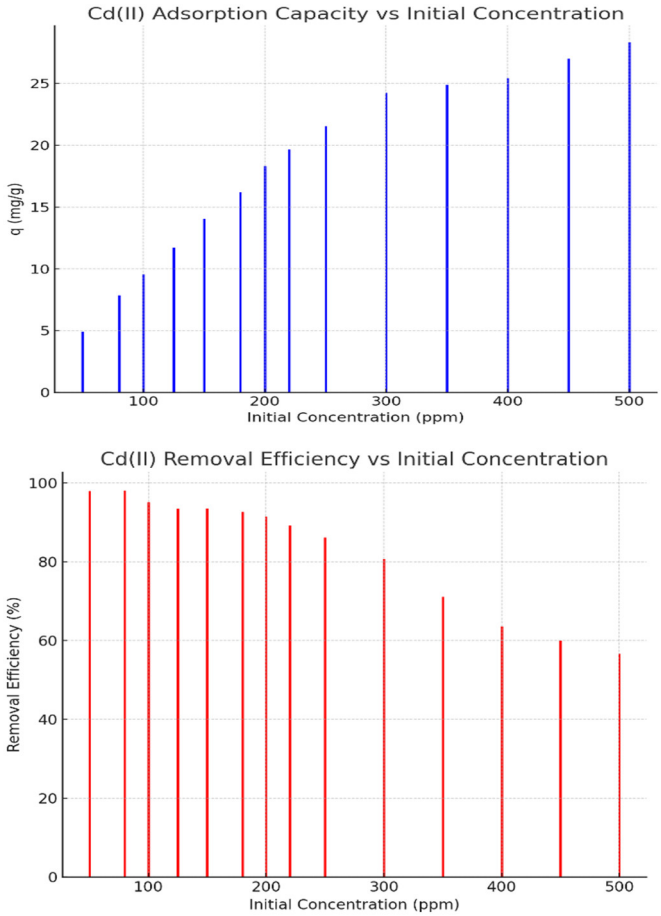

Figure 13. Adsorption Capacity and Removal Efficiency of BC/CS12 Composite Material for Cd(II) Ion Removal at Different Initial Concentrations

The BC/CS12 composite material demonstrates high efficiency in adsorbing and removing Cd(II) ions. The results from the adsorption capacity graph show that as the concentration of Cd(II) ions in the solution increases, the amount of ions adsorbed onto the BC/CS12 material also increases. However, the growth of the adsorption capacity does not continue to rise significantly once the concentration of Cd(II) exceeds a certain threshold, indicating that the adsorption sites are becoming saturated. For the removal efficiency, BC/CS12 maintains a very high removal rate, ranging from 85% to 90%, even when the concentration of Cd(II) ions in the solution changes from low to high. This proves that BC/CS12 not only has excellent adsorption capacity but also maintains its effectiveness in removing Cd(II) ions at various concentrations. With these results, BC/CS12 is a promising material for heavy metal ion wastewater treatment, especially for Cd(II).

3.4.2.2. Effect of time on the adsorption efficiency of metal ions of BC/CS12 material

The results from the chart show that the adsorption efficiency of Cd(II) ions on the BC/CS material increases with contact time. After about 10 minutes, the adsorption efficiency starts to rise and reaches 96.6% after 100 minutes. After 120 minutes, the adsorption efficiency remains stable, indicating that BC/CS has a strong adsorption capacity for Cd(II) throughout the experiment. This can be explained by the interaction of functional groups on the BC/CS surface with Cd(II) ions, enhancing the adsorption capacity. However, after reaching a certain level, the efficiency does not increase further, indicating that the BC/CS material has become saturated and cannot adsorb more Cd(II) ions under the experimental conditions.

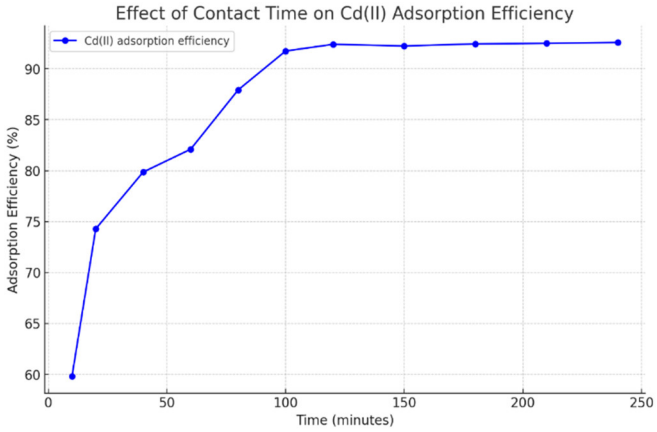

Figure 14. Effect of Contact Time on the Adsorption Efficiency of Cd(II) Ions on BC/CS Composite

3.4.2.3. Effect of pH on the adsorption efficiency of Cd metal ions of the material

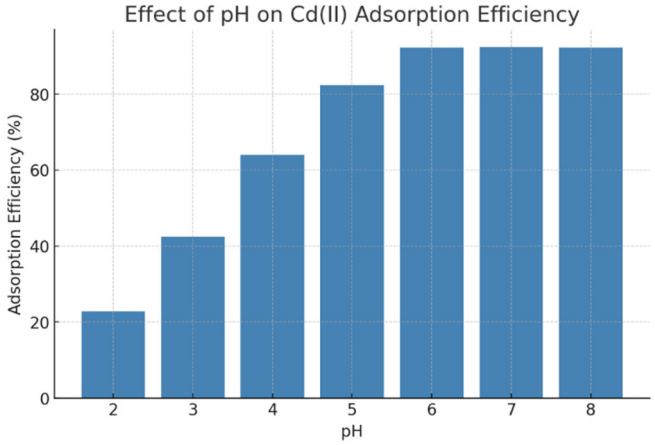

Figure 15. Effect of pH on Cd(II) Adsorption Efficiency

The bar chart above illustrates the effect of pH on the adsorption efficiency of Cd(II) by BC/CS12 material. As observed, the adsorption efficiency increases significantly as the pH value increases from 2 to 5, with a peak observed at pH 5, where the adsorption efficiency reaches 92.24%. The efficiency continues to remain high from pH 5 to pH 8, indicating that the BC/CS12 material maintains good efficiency for Cd(II) adsorption within this pH range. This suggests that the material performs optimally at slightly acidic to neutral pH levels, which could be useful for real-world applications in treating wastewater with varying pH conditions.

The chart shows that the optimal pH for achieving the highest adsorption efficiency of Cd(II) on the BC/CS12 material is pH 5. At this pH value, the adsorption efficiency reaches 92.24%, indicating that the BC/CS12 material performs best in slightly acidic conditions. As the pH increases from 5 to 8, the adsorption efficiency remains stable at a high level, suggesting that the material maintains effective adsorption within this pH range.

3.4.2.4. Adsorption Isotherms

In the **Langmuir isotherm for Cd(II)** (on the left), we can observe a linear relationship between Ce (concentration of Cd(II) in solution) and qe (amount of Cd(II) adsorbed per unit mass of adsorbent). The fitted equation is $y = 0.0474x + 0.6075$, with an R^2 value of 0.9902. This high R^2 value indicates a strong fit, suggesting that the adsorption of Cd(II) on the adsorbent follows the Langmuir model, which assumes monolayer adsorption on a surface with a finite number of identical sites. This indicates that the adsorption sites are homogeneously distributed across the adsorbent surface. The **Freundlich isotherm for Cd(II)** (on the right) also shows a linear relationship when plotted as log(qe) versus log(Ce). The fitted equation is $y = 0.3907x + 0.5513$, with an R^2 value of 0.9066. The R^2 value is slightly lower than that of the Langmuir model, suggesting that the adsorption process might also have some degree of heterogeneity, as the Freundlich model is generally used to describe adsorption on heterogeneous surfaces. In conclusion, both isotherm models fit the data, with the Langmuir model showing a slightly better fit for Cd(II) adsorption on the BC/CS material. The Langmuir isotherm's R^2 value indicates a well-defined adsorption process with high affinity and capacity for Cd(II) on the material.

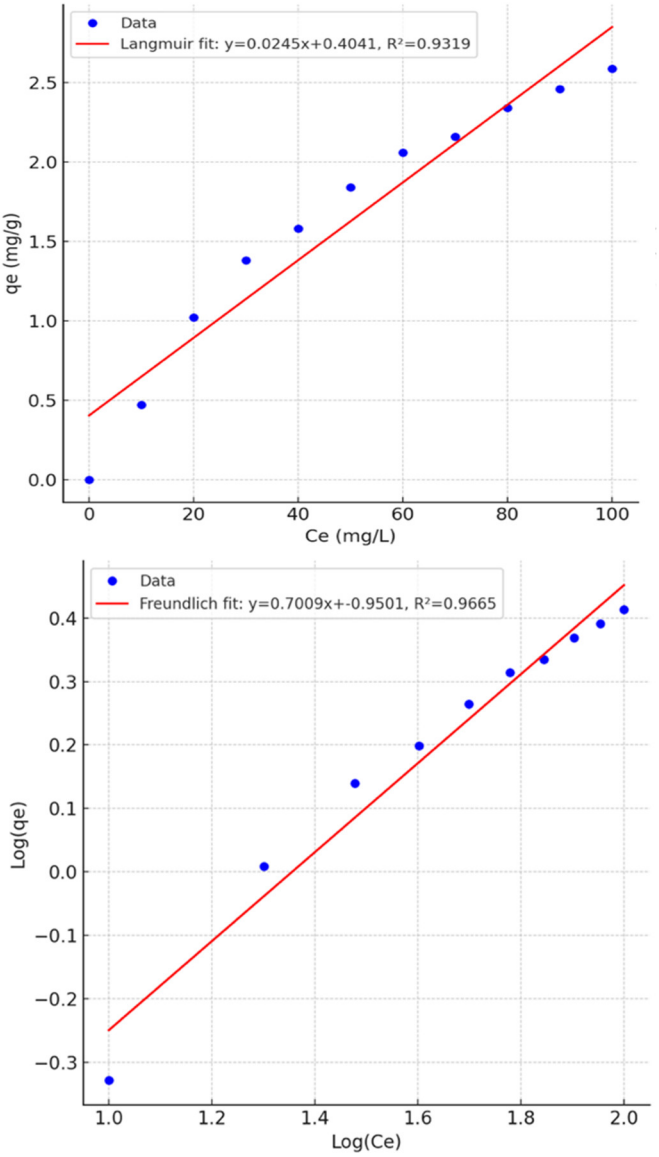

Figure 16. The adsorption isotherm of Cd(II) ion on BC/CS according to the concentration of adsorbent dosage: Langmuir and Freundlich

3.4.2.5. Evaluation of Cd(II) adsorption capacity of BC/CS by EDX-SEM method

The results from the EDX-SEM method, as shown in Figures 17, 18, and 19, indicate the Cd(II) adsorption capacity on the BC/CS composites. Specifically, the mass percentage of Cd(II) adsorption on the materials BC/CS11, BC/CS12, and BC/CS13 are 0.23 wt.%, 0.24 wt.%, and 0.21 wt.%, respectively. These results show that BC/CS12 has the highest Cd(II) adsorption capacity among the three materials, with an adsorption of 0.24 wt.%, suggesting that BC/CS12 has optimal surface properties for adsorbing Cd(II) ions compared to BC/CS11 and BC/CS13. Both BC/CS11 and BC/CS13 have relatively lower Cd(II) adsorption capacities, with values of 0.23 wt.% and 0.21 wt%, respectively, indicating that their surface properties or chemical interactions with Cd(II) ions are not as optimal as BC/CS12. Although the differences between the materials are not large, BC/CS12 still demonstrates the highest adsorption efficiency. This highlights the importance of optimizing composite materials to improve the removal of heavy metals such as Cd(II) in wastewater treatment.

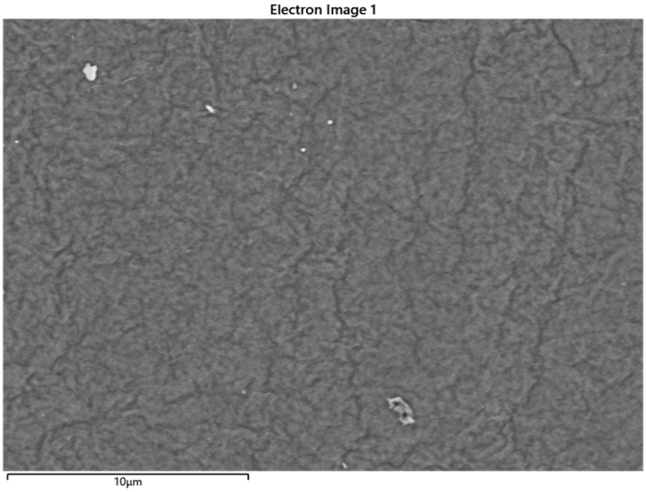

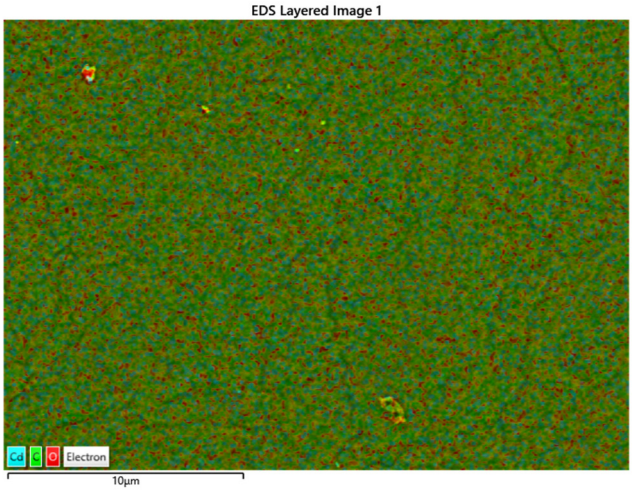

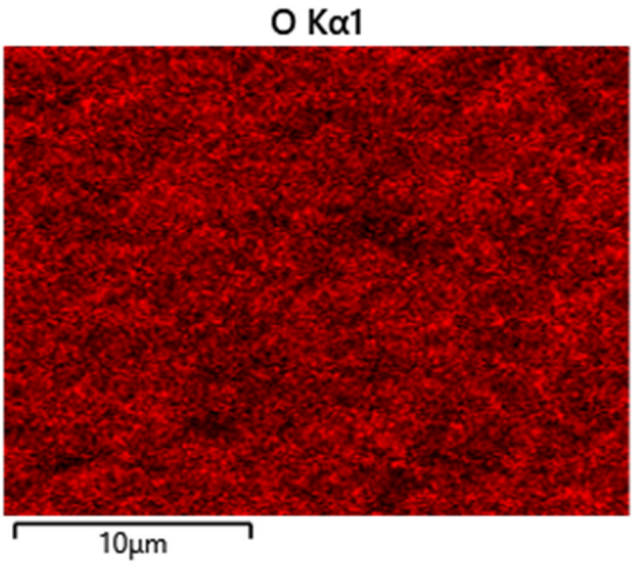

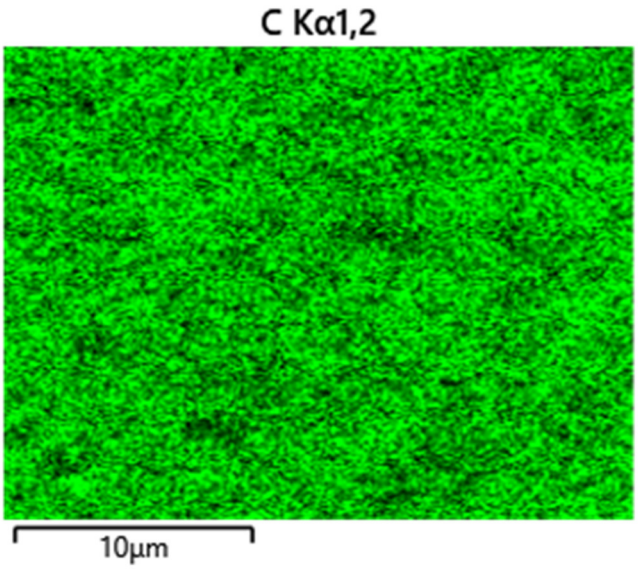

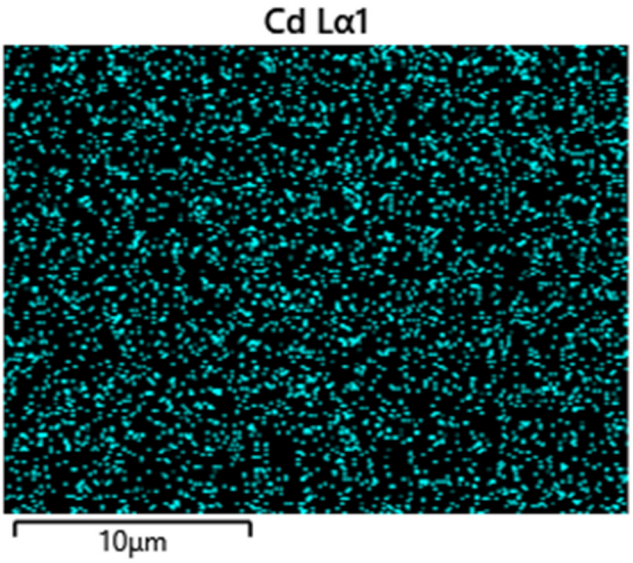

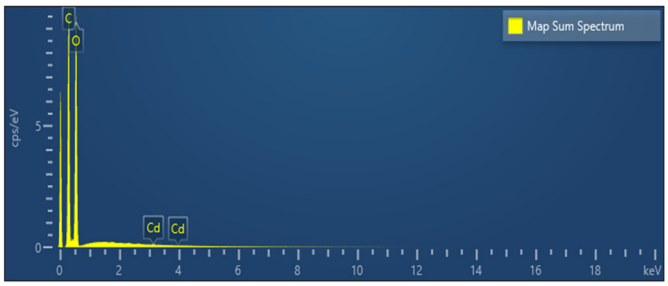

Map Sum Spectrum				
Element	**Line Type**	**Weight %**	**Weight % Sigma**	**Atomic %**
C	K series	46.50	0.16	53.75
O	K series	53.27	0.16	46.22
Cd	L series	0.23	0.05	0.03
Total		100.00		100.00

Figure 17. Cd(II) adsorption capacity of BC/CS11 by EDX-SEM method

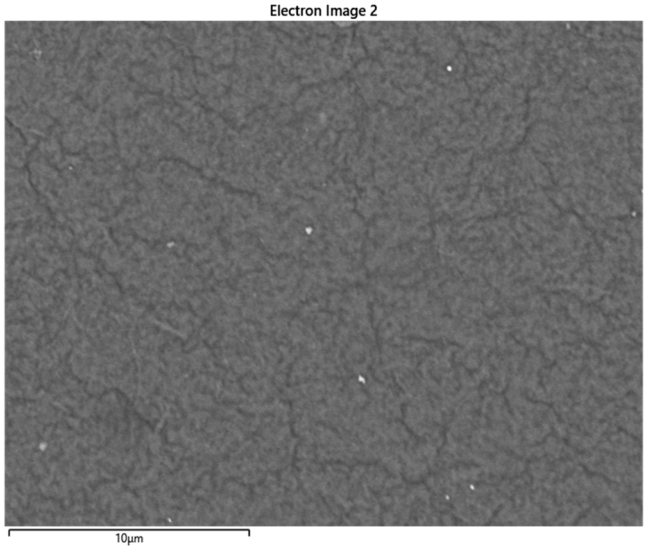

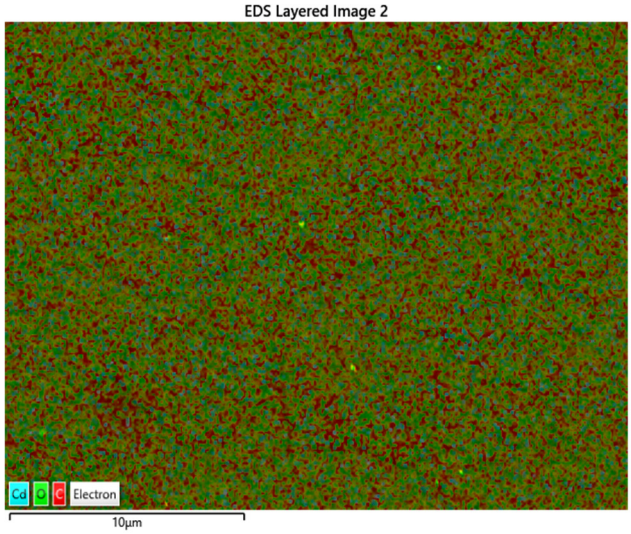

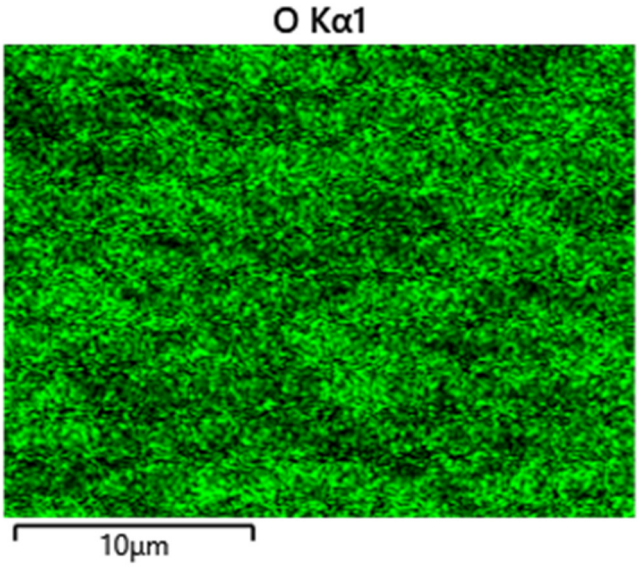

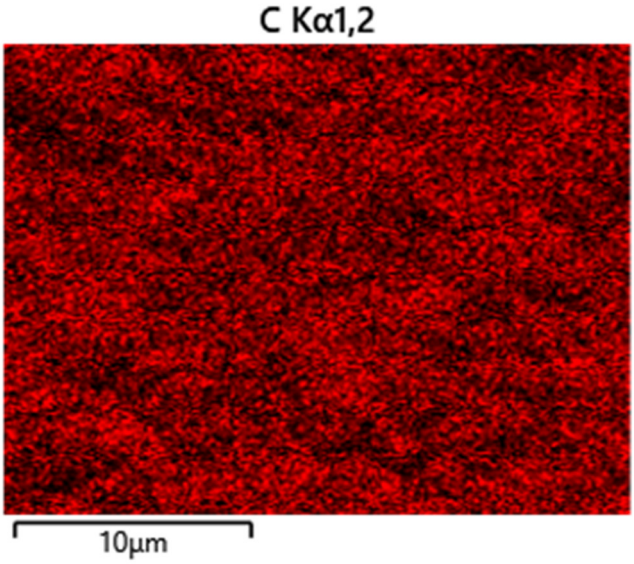

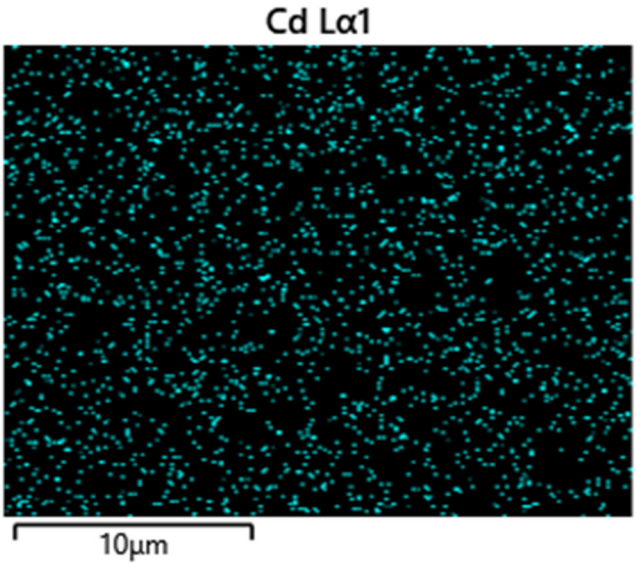

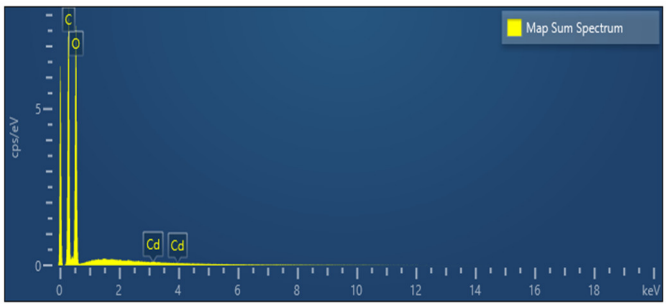

Map Sum Spectrum				
Element	**Line Type**	**Weight %**	**Weight % Sigma**	**Atomic %**
C	K series	47.10	0.24	54.35
O	K series	52.66	0.24	45.62
Cd	L series	0.24	0.08	0.03
Total		100.00		100.00

Figure 18. Cd(II) adsorption capacity of BC/CS12 by EDX-SEM method

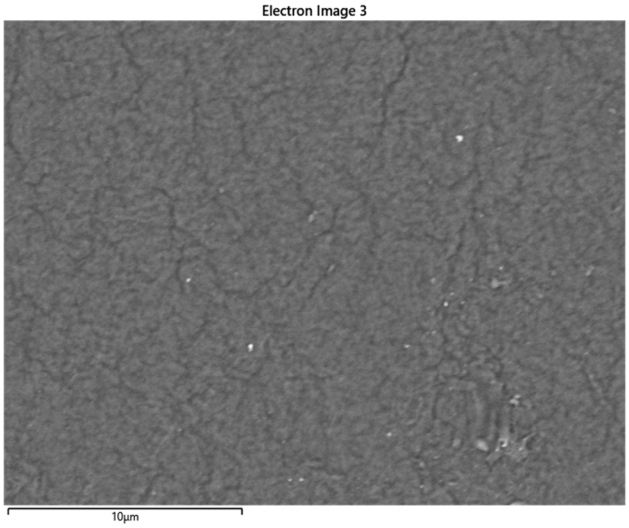

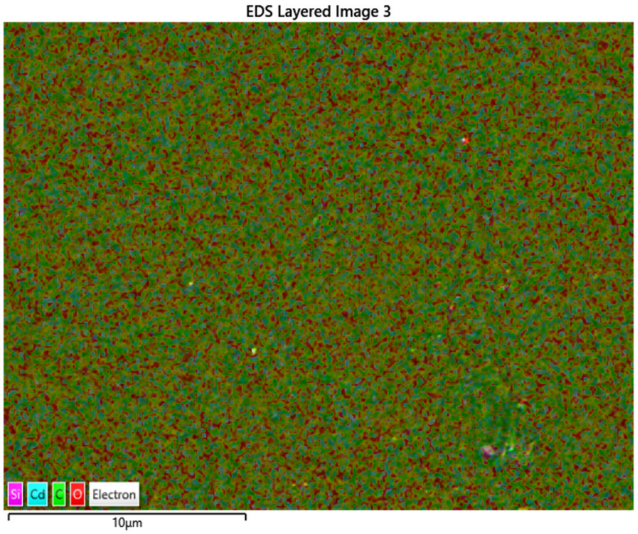

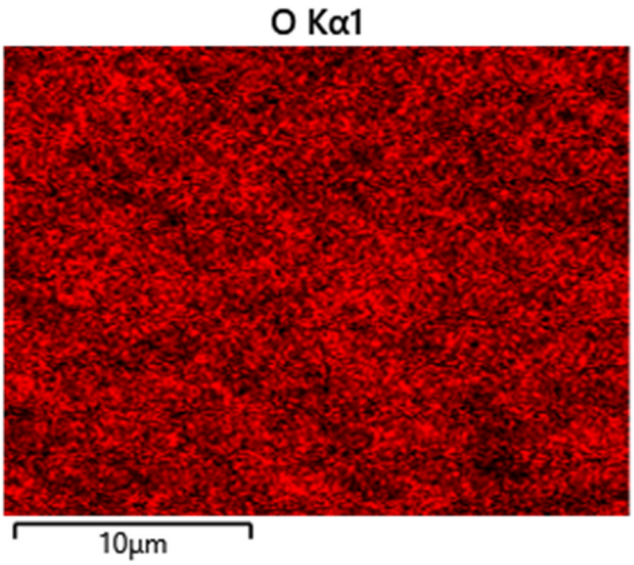

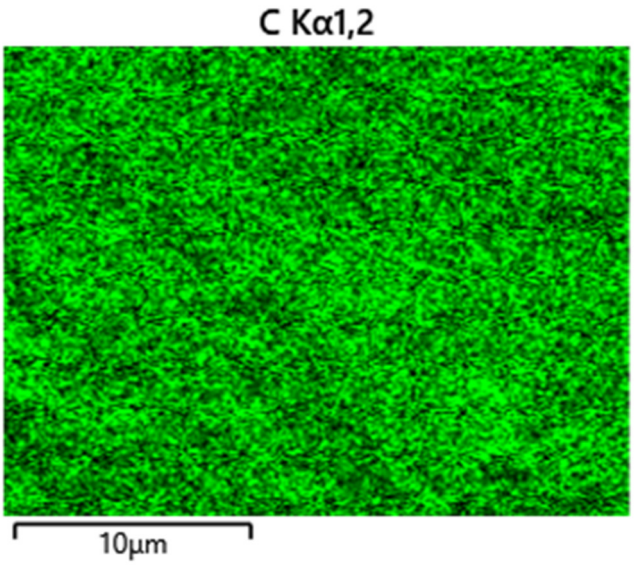

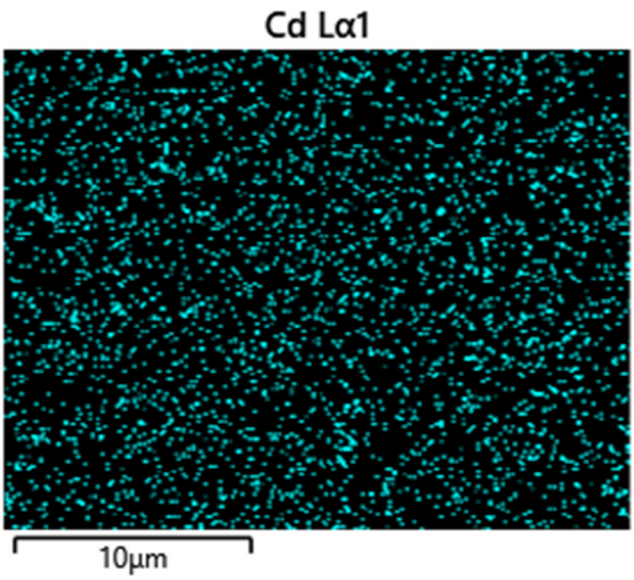

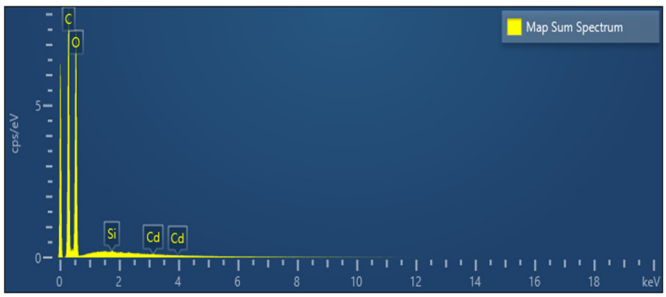

Map Sum Spectrum				
Element	**Line Type**	**Weight %**	**Weight % Sigma**	**Atomic %**
C	K series	47.10	0.20	54.36
O	K series	52.60	0.20	45.57
Si	K series	0.08	0.02	0.04
Cd	L series	0.21	0.06	0.03
Total		100.00		100.00

Figure 19. Cd(II) adsorption capacity of BC/CS13 by EDX-SEM method

4. CONCLUSION

The BC/CS12 composite membrane, with an optimal ratio of BC and CS, demonstrated high adsorption efficiency for heavy metals such as Pb(II) and Cd(II), especially for Pb(II) with a removal efficiency of up to 98.58% at a concentration of 500 ppm. For Cd(II), BC/CS12 also showed excellent adsorption efficiency, reaching 92.50% at 500 ppm concentration. EDX-SEM analysis revealed that the Cd(II) adsorption capacity of BC/CS12 was 0.24 wt.%, the highest among the BC/CS samples, including BC/CS11 and BC/CS13 (with adsorption capacities of 0.23 wt.% and 0.21 wt.% respectively). The BC/CS12 membrane not only demonstrated high adsorption efficiency but also exhibited good mechanical strength and reusability, making it an ideal material for heavy metal wastewater treatment. With these promising results, BC/CS12 has great potential for applications in wastewater treatment and environmental protection. However, to enhance its adsorption capacity and reusability, future studies could focus on optimizing the composite structure, such as increasing the surface area of BC/CS or incorporating other active components. Additionally, evaluating the adsorption capacity for other heavy metals like Cr(III), Cr(VI), and As(V) will be a promising direction to expand the applications of this material.

ACKNOWLEDGEMENT

The authors express gratitude to the Faculty of Chemical Technology at Hanoi University of Industry (HaUI) for the financial support provided in conducting this research.

Data Availability: All relevant data supporting the findings of this study are available within the article.

The authors confirm that there are no conflicts of interest associated with the publication of this paper.

REFERENCES

[1]. S.Y. Quek, D.A.J. Wase, C.F. Forster, "The use of sago waste for the sorption of lead and copper," *Water SA*, 24, 251-256, 1998.

[2]. K. Vaaramaa, J. Lehto, "Removal of metals and anions from drinking water by ion exchange," *Desalination*, 155 (2), 157-170, 2003.

[3]. H. Zhang, X. Zhao, J. Wei, F. Li, "Sorption behavior of cesium from aqueous solution on magnetic hexacyanoferrate materials," *Nucl. Eng. Desalinat.*, 275, 322-328, 2014.

[4]. X. Hu, Y. Li, Y. Wang, et al., "Adsorption kinetics, thermodynamics and isotherm of thiacalix [4] arene-loaded resin to heavy metal ions," *Desalination* 259, 76-83, 2010.

[5]. M. Cerna, E. Monitoring, "Use of solvent extraction for the removal of heavy metals from liquid wastes," *Environ. Monit. Assess.*, 34, 1-6, 2014.

[6]. R. Coskun, C. Soykan, M. Sacak, "Removal of some heavy metal ions from aqueous solution by adsorption using poly (ethylene terephthalate)-g-itaconic acid/ acrylamide fiber," *Reactive Funct. Polymers,* 66, 599-608, 2006.

[7]. R.K. Rattan, S.P. Datta, P.K. Chhonkar, K. Suribabu, A.K. Singh, " Long-term impact of irrigation with sewage effluents on heavy metal content in soils, crops and groundwater - a case study," *Agric. Ecosyst. Environ.*, 109, 310-322, 2005.

[8]. S. Mahgoub, P. Samaras, "Nanoparticles from biowastes and microbes: Focus on role in water purification and food preservation," in *2nd International Conference on Sustainable Solid Waste Management,* 2014.

[9]. Q. Li, S. Mahendra, D.Y. Lyon, L. Brunet, M.V. Liga, D. Li, P.J. Alvarez, "Antimicrobial nanomaterials for water disinfection and microbial control: potential applications and implications," *Water Res.*, 42, 4591-4602, 2008.

[10]. B. Liu, D. Wang, G. Yu, X. Meng, "Adsorption of heavy metal ions, dyes and proteins by chitosan composites and derivatives - A review," *J. Ocean Univ. China*, 12, 500-508, 2013.

[11]. U. Perera, N. Rajapakse, "Chitosan Nanoparticles: Preparation, Characterization, and Applications," *Seafood Processing By-Products*, Springer, 371-387, 2014.

[12]. Y. Sharma, V. Srivastava, V. Singh, S. Kaul, C. Weng, "Nano-adsorbents for the removal of metallic pollutants from water and wastewater," *Environ. Technol.,* 30, 583-609, 2009.

[13]. M. Vakili, M. Rafatullah, B. Salamatinia, A.Z. Abdullah, M.H. Ibrahim, K.B. Tan, Z. Gholami, P. Amouzgar, "Application of chitosan and its derivatives as adsorbents for dye removal from water and wastewater: A review," *Carbohydrate Polymers,* 113, 115-130, 2014.

[14]. G. Crini, P. M. Badot, "Application of chitosan, a natural amino polysaccharide, for dye removal from aqueous solutions by adsorption processes using batch studies: A review of recent literature," *Prog. Polym. Sci.*, 33 (4), 399-447, 2008.

[15]. D.S. Rajawat, A. Kardam, S. Srivastava, S.P. Satsangee, "Nanocellulosic fiber- modified carbon paste electrode for ultra trace determination of Cd (II) and Pb (II) in aqueous solution," *Environ. Sci. Pollut. Res.*, 20, 3068–3076, 2013.

[16]. R. Muzzarelli, "Nanochitins and nanochitosans, paving the way to eco-friendly and energy-saving exploitation of marine resources," *Polymer science: A comprehensive reference*, 10, 153-164, 2012.

[17]. Y.C. Chang, S.W. Chang, D.H. Chen, "Magnetic chitosan nanoparticles: Studies on chitosan binding and adsorption of Co (II) ions," *React. Funct. Polym.,* 66, 335-341, 2006.

[18]. S. Hokkanen, E. Repo, T. Suopajärvi, H. Liimatainen, J. Niinimaa, M. Sillanpää, "Adsorption of Ni (II), Cu (II) and Cd (II) from aqueous solutions by amino modified nanostructured microfibrillated cellulose," *Cellulose*, 21, 1471-1487, 2014.

[19]. Suman, A. Kardam, M.Gera, V. Jain, "A novel reusable nanocomposite for complete removal of dyes, heavy metals and microbial load from water based on nanocellulose and silver nano-embedded pebbles," *Environ. Technol.,* 36, 706-714, 2015.

[20]. F.C. Wu, R.L. Tseng, R.S. Juang, "Enhanced abilities of highly swollen chitosan beads for color removal and tyrosinase immobilization," *J. Hazard. Mater.*, 81,167-177, 2001.

[21]. M. S. Chiou, P. Y. Ho, H. Y. Li, "Adsorption of anionic dyes in acid solutions using chemically cross-linked chitosan beads," *Dye Pigment*, 60 (1), 69-84, 2004.

[22]. W. S. W. Ngah, S. Fatinathan, "Chitosan flakes and chitosan-GLA beads for adsorption of p-nitrophenol in aqueous solution," *Colloids Surf.,* A 277 (1-3), 214-222, 2006.

[23]. S. Islam, M. Shahid, F. Mohammad, "Green chemistry approaches to develop antimicrobial textiles based on sustainable biopolymers - A review," *Ind. Eng. Chem. Res.*, 52, 5245-5260, 2013.

[24]. J. Zhou, C. Chang, R. Zhang, L. Zhang, "Hydrogels prepared from unsubstituted cellulose in NaOH/urea aqueous solution," *Macromole Biosci*., 7, 804-809, 2007.

[25]. M. A. S. Azizi Samir, F. Alloin, A. Dufresne, "Review of recent research into cellulosic whiskers, their properties and their application in nanocomposite field," *Biomacromolecules*, 6, 612-626, 2005.